JOURNAL OF SPACECRAFT AND ROCKETS
Vol. 42, No. 3, May–June 2005

Trajectory and System Analysis for Outer-Planet Solar Electric Propulsion Missions

Byoungsam Woo,* Victoria L. Coverstone,† and John W. Hartmann*
University of Illinois at Urbana–Champaign, Urbana, Illinois 61801
and
Michael Cupples‡
Science Applications International Corporation, Huntsville, Alabama 35806

Outer-planet mission and systems analyses are performed using three next-generation solar-electric ion thruster models. The impact of variations in thruster model, flight time, launch vehicle, propulsion and power systems characteristics is investigated. All presented trajectories have a single Venus gravity assist and maximize the delivered mass to Saturn or Neptune. The effect of revolution ratio—the ratio of Venusian orbital period to the flight time between launch and flyby dates—is also discussed.

Introduction

WITH the success of the Deep Space 1 mission, solar electric propulsion systems[1,2] (SEPS) were ushered into the mainstream of propulsion system candidates for various interplanetary missions.[3,4] The long-duration, high-efficiency operation of SEPS allows new ways to explore the inner and outer solar system and enables missions that can be difficult and expensive to reach with chemical propulsion systems.

This paper provides a parametric survey of a set of mission and system factors that affect the delivered mass for SEPS vehicles considered for unmanned outer-planet science missions. The mission characteristics examined in this paper include delivered mass to the destination as a function of launch vehicle, total flight time, and gravity-assist timing. Each of these factors plays a significant role in the resultant value of the optimized SEPS performance metrics.

To facilitate a systematic examination of SEPS performance, a baseline SEPS vehicle and mission are chosen. The basic performance requirements of this system are derived from the NRA-01-OSS-01.[5] Table 1 provides the baseline mission and vehicle definitions.

This paper also provides the details of a single Venus gravity assist to Saturn and Neptune. In exploring the outer solar system planets, a planetary gravity assist (GA) has commonly been used because one or more GAs have the potential to save propellant, reduce time of flight (TOF), or both. Because of these advantages, many previous interplanetary missions (e.g., Mariner 10, Voyager I, II, Galileo, Cassini, and NEAR) exploited the GA.[6] In this study, a single Venus GA is included in all Earth–Venus–Saturn (EVS) and Earth–Venus–Neptune (EVN) trajectories.

The trajectories presented are generated using SEPTOP (Solar Electric Propulsion Trajectory Optimization Program),[7] which calculates a trajectory that maximizes the delivered mass to a destination. That delivered mass can include the scientific payload along with aerocapture equipment, propulsion system, and supporting bus. Given equal mission and systems assumptions for a SEPS vs chemical mission comparison (except for capture method), a SEPS/aerocapture combination generally can deliver greater payload to a set destination (assuming an attained "small enough" aerocapture mass fraction) than a chemical mission. However, early tradeoff results would probably indicate lower system reliability and higher system development cost for aerocapture when compared with a chemical capture.

Presented as AAS Paper 2003-242 at the AAS/AIAA 13th Space Flight Mechanics Meeting, Ponce, PR, 9–13 February 2003; received 11 December 2003; revision received 20 May 2004; accepted for publication 20 May 2004.

*Graduate Research Assistant, Department of Aeronautical and Astronautical Engineering, 104 S. Wright Street.
†Associate Professor, Department of Aeronautical and Astronautical Engineering, 104 S. Wright Street. Associate Fellow AIAA.
‡Lead Systems Engineer, In-Space Technology Assessment.

Optimization

The trajectory optimization problem with variable thrust and thrust direction has been previously investigated.[7,8] The problem is typically formulated to optimize a number of parameters, but in this research the final delivered mass to Saturn or Neptune is maximized.

SEPTOP was used for the mission analysis of Deep Space 1 at the Jet Propulsion Laboratory. SEPTOP is a two-body, sun-centered, low-thrust trajectory optimization program for preliminary mission feasibility studies that provides relatively accurate performance estimates. The program determines a numerical solution to a two-point boundary-value problem that satisfies intermediate boundary constraints. In SEPTOP, the user estimates initial conditions, then uses a shooting method to integrate the trajectory from an initial time to final time. SEPTOP computes an error at the final time and uses it to correct the estimate of the initial conditions. This process is repeated until the error becomes smaller than the prescribed tolerance.[9] The required inputs are TOF, nominal epoch, array power at Earth departure P_0, maximum power into power processing unit (PPU), flyby radius, and launch-vehicle specifications. SEPTOP can model variable thrust and mass flow rate as a function of power into the PPU. The power generated from a solar array is modeled as a function of the spacecraft's distance from the sun. Thruster and solar array models are therefore also required as inputs.

Many parameters remain free to be optimized, for example, launch date, launch energy (C_3), flyby dates, and initial values for Lagrange multipliers. Trajectories generated with SEPTOP represent locally optimal solutions in the parameter space. It is therefore possible for multiple locally optimal solutions to exist possessing similar SEPTOP input parameters. The characteristics of such solutions are explained and categorized using the Saturn and Neptune example missions. Trajectories are first categorized by launch opportunity. In some situations, two locally optimal trajectories with similar inputs exist: one with a launch opportunity that occurs early on in the given launch window (early) and the other with a late launch opportunity (late). Second, the trajectories are categorized by their revolution ratio (R ratio). The R ratio is the number of Venus revolutions for one revolution of a spacecraft around the sun. For instance, a 3:1 R ratio is one where roughly three Venus years occur

Table 1 Baseline mission and system definition

Parameter	Definition
Target planet	Saturn and Neptune
Reference	1400 kg (Saturn)
Payload	850 kg (Neptune)
Delta-V	$\leq$14 km/s for reference payloads
Launch vehicle	Delta IV M, Atlas V M
Power	30 kWe at 1 AU EOL; 25 kWe max into PPU
Thrusters	4 thrusters + 1 spare 6.1 kWe at 3900 s I_{sp}
Grids	Molybdenum grids
PPU	4 PPUs + 1 spare Cross strapping PPUs SOA heat pipe radiators
Tank fraction	5%
Propellant	Supercritical Xe

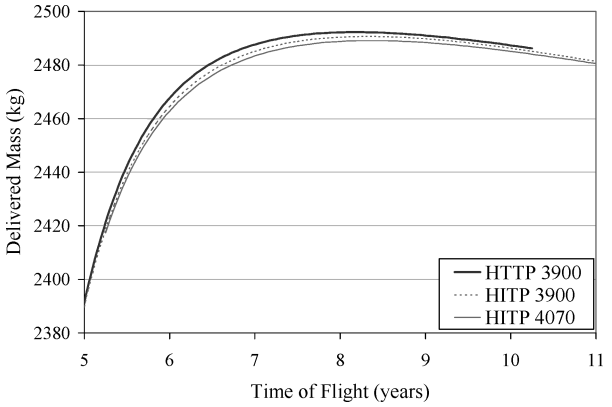

Fig. 1 Delivered mass vs TOF: EVS mission, 3:1 R ratio, late type, Delta-IV 4240.

during the period from launch to flyby of Venus by the spacecraft. In this paper, the performance of trajectories for each launch opportunity type and R ratio is investigated. TOF is one of the main mission design drivers. Determining the minimum TOF trajectory that delivers the reference payload is commonly of interest.

Solar Electric Propulsion System

The primary spacecraft propulsion sources in this study are near-term next-generation ion propulsion systems. Three different models are compared for their performance: high-thrust-to-power (HTTP) I_{sp} 3900 s, high-I_{sp}-to-power (HITP) I_{sp} 3900 s, and HITP I_{sp} 4070 s (Ref. 10). The definition of the performance of a trajectory is the delivered mass for a given TOF. The I_{sp} values used in these engine descriptions are the values at each respective engine's maximum operating power P_{max} of 6.1 kWe. The minimum operating power P_{min} is 1.11 kWe for all three thruster models. The thrust and mass flow rate for the thruster models are given in Patterson et al.[10] Of the three models, the HTTP I_{sp} 3900-s thruster has the largest thrust and mass flow rate for operation between the given P_{min} and P_{max}.

Delivered mass is first investigated for the three thruster models in order to determine the best performing thruster model for the EVS and EVN missions. Figure 1 shows the delivered mass vs TOF for a late type, 3:1 R ratio, EVS mission using three thruster models. Figure 2 shows the performance for a late type, 2:1 R ratio, EVN mission. Among the three models, the HTTP I_{sp} 3900-s model consistently delivered more mass to the destination. Therefore, the HTTP I_{sp} 3900-s model is selected as the default thruster for much of the analysis in this paper. The objective of the thruster comparison is to determine a default thruster model for this paper, not to decide which throttling mode is generally superior. Also, during an actual

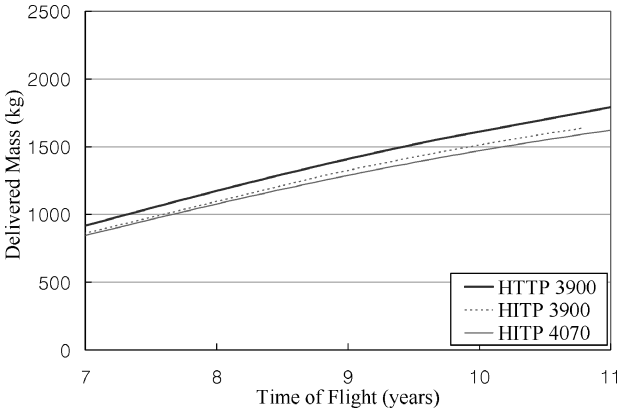

Fig. 2 Delivered mass vs TOF: EVN mission, 2:1 R ratio, late type, Delta-IV 4240.

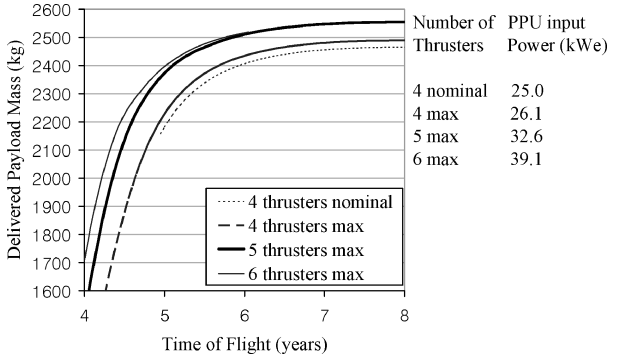

Fig. 3 Delivered payload mass dependence on number of thruster for EVS mission, HTTP 3900 thruster, 3:1 R ratio, Atlas 431.

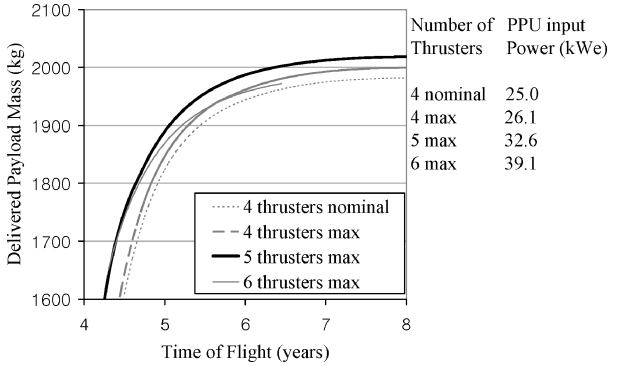

Fig. 4 Delivered payload mass dependence on number of thruster for EVS mission, HTTP 3900 thruster, 3:1 R ratio, Delta-IV 4450.

mission a thruster can be operated in different throttling modes (high thrust or high I_{sp}) depending on the power available at any given moment; however, this is dual mode of operation is not considered here.

The delivered payload mass vs TOF plots in Figs. 3 and 4 show the delivered payload mass sensitivity of the SEPS vehicle to the number of thrusters. The definition of the delivered payload mass is the delivered mass to the destination minus the bus mass. In this analysis, the PPU input power increased as the number of thrusters is increased to utilize all of the thrusters. The PPU input power at Earth departure for representative cases is shown in Figs. 3 and 4. The analysis includes two launch vehicles: the Atlas 431 and the Delta-IV 4450. From Fig. 3, the delivered payload mass by an Atlas 431 increases with increasing power and increasing number of thrusters but decreases as the number of thrusters increases to six. Overall, five thrusters appear to provide superior performance, whereas six thrusters provide a small improvement in TOF below

five years. Similar trends hold true for the Delta 4450 as displayed in Fig. 4, but there appears to be no advantage in TOF for six thrusters.

Power System

Large, high-efficiency, multijunction GaAs arrays provide propulsion power and vehicle housekeeping power. An articulation of the arrays in one axis relative to the sun provides array feathering to control array temperature and to prevent the solar flux from exceeding a maximum allowable solar flux on the arrays during the high solar intensity portion of the trajectory (e.g., spacecraft at <1 AU from the sun during Venus gravity assist). Prolonged solar-array operation at high temperatures and array exposure to solar radiation degrade the efficiency of the photovoltaic cells. For this analysis a cell efficiency degradation factor of 2% average per year is applied. In addition, sizing the array area by 5% larger than required for the 30-kWe array output requirement provides further design margin. Able Engineering, a solar-array manufacturer, provided Ultra-Flex array modeling characteristics. The Ultra-Flex model represents the present state of the art in lightweight solar-array technology. This model can be represented as solar flux approximately dropping off as $1/r^2$, yet also includes effects for low-intensity light and low temperature (LILLT).[11] The LILLT modeling effects make a significant impact in the overall performance expected from the array. The housekeeping power is assumed to be covered by the 5 additional kWe from the array.

A PPU[12] converts power from the solar array and delivers electrical power at proper voltage and current to the thruster array. PPU efficiency is less than 100% (varying as a function of PPU input power), which results in losses when processing power from the solar array. Power to the thrusters is provided by the PPU; therefore, the power generated by the solar array needs to be greater than the number of thrusters multiplied by $P_{\max}$ if multiple thrusters are to be operated at their maximum power.

To observe the effect of the power system characteristics on a mission, the array power is varied in an EVS and an EVN mission. Figure 5 shows the array power at Earth departure P_0 vs delivered mass. This figure illustrates that Saturn can be reached with less P_0 for a given delivered mass than Neptune. This result also provides a design reference for the solar-array sizing. If an optimal P_0 to deliver the most payload mass exists, it can be found once the power, propulsion, and bus sizing is computed for the range of P_0.

Figure 6 displays the delivered payload mass in an EVN mission. Assumptions include the following: 11.3-year TOF, four thrusters, 25 kWe for maximum PPU input power, 2:1 R ratio, and variable P_0. A minimum P_0 of approximately 26.3 kWe allows the 850-kg reference payload to be delivered to Neptune in 11.3 years. The delivered payload mass increases with P_0 (yet with diminishing returns) until reaching a maximum at approximately 48.2 kWe. Beyond 48.2 kWe, the delivered payload mass begins to decrease because of the SEPS propulsion system maximum power level remaining constant at 25 kWe, but the array, array support structure, and

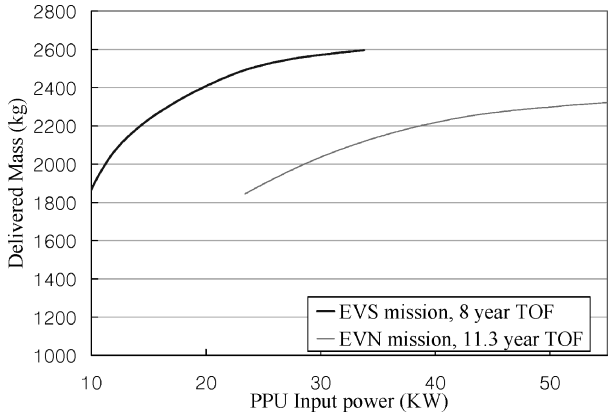

Fig. 5 Delivered mass vs P_0 variation: EVS mission (8-year TOF, 3:1 R-ratio) and EVN mission (11.3-year TOF, 2:1 R ratio), Delta-IV 4240.

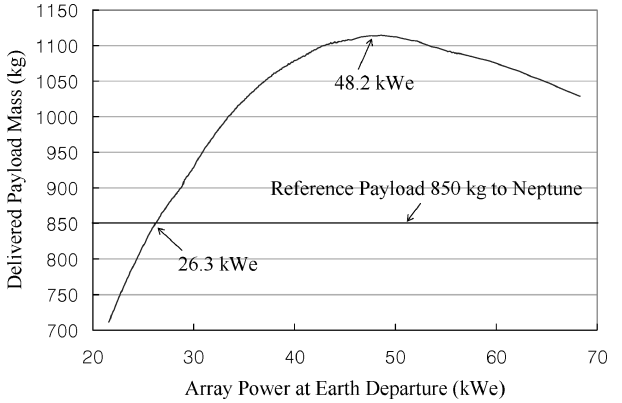

Fig. 6 Delivered payload mass dependence on array power for EVN mission, Delta-IV 4240.

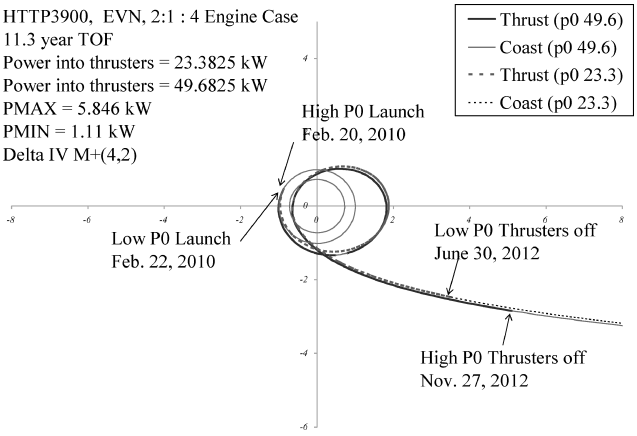

Fig. 7 Trajectories for two P_0 levels: EVN mission, 11.3-year TOF, 2:1 R ratio, Delta-IV 4240.

primary bus structure masses all continue to increase. The reference array power of 30 kWe, near the minimum value of 26.3 kWe, provides little delivered payload (or dry mass) margin. Yet, the margin in payload gained from an increase in array power must be weighed against a significant increase in actual array cost (from inherently high specific cost \$/kg) in larger, more complex arrays, and in new, large array development risks.

Next, trajectories for an EVN mission that have the same TOF, launch type, and R ratio but different P_0 are shown in Fig. 7. The trajectories are almost the same, but the thrusting phase is longer in the higher P_0 trajectory. This is because in the high P_0 trajectory the spacecraft has power available to it—greater than $P_{\min}$ to operate a single thruster—at farther distances from the sun. This difference results in the higher P_0 trajectory providing more delivered mass to the destination because a lower C_3 is required for the trajectory. When given the option, the best performing trajectories tend to favor the higher efficiency SEPS over the less efficient launch vehicle to provide energy increase for the trajectory.

Launch Vehicle

The choice of launch vehicle significantly impacts mission cost, mission reliability, and delivered mass performance. This factor is explicitly brought to the foreground given that the trajectory optimization process adopted for this analysis ties the launch-vehicle delivery capability directly into the optimization process. Generally, with all other assumptions equivalent, the larger launch vehicle will deliver the greater mass to a given destination; however, the mission goal is to deliver the reference payload to the destination for a minimum cost. Thus, an optimization process must ultimately be undertaken to find the best compromise between launch-vehicle cost and delivery of reference payload. This paper does not examine this optimization process but does look at the question of predicted

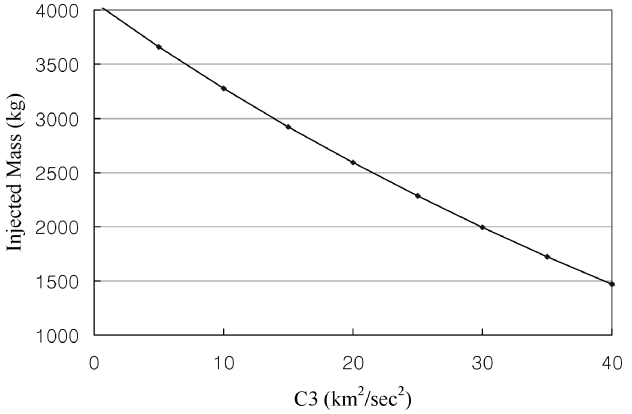

Fig. 8 Injected mass vs C_3 for Delta-IV 4240.

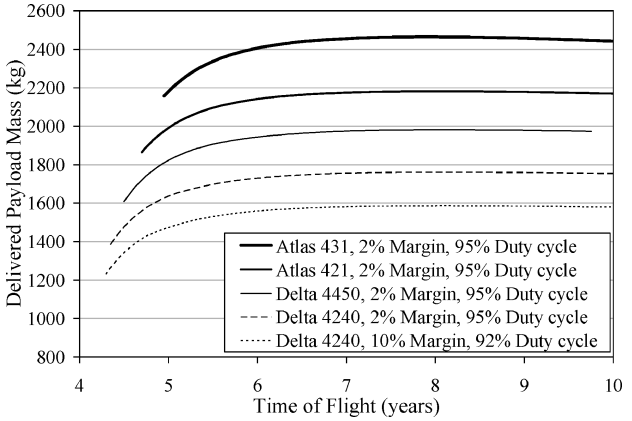

Fig. 9 Performance dependence on launch vehicles for an EVS mission.

performance over a range of TOF for several current launch vehicles. This paper examines Delta-IV[13] medium and Atlas-V[14] medium-launch vehicles.

Figure 8 provides the Delta-IV 4240 launch-vehicle data in the form of injected mass to a particular launch C_3. The SEPTOP trajectory optimization tool uses the injected mass vs C_3 constraint to enforce the specific performance characteristics of given launch vehicles. With this constraint, however, SEPTOP can only search a range of C_3 (or injected mass) that satisfies the constraint. This can lead to an undesirable result of decreasing performance for increasing injected mass, especially when the SEPS and power system are incapable to thrust the increased injected mass within a given TOF. If there is no launch-vehicle constraint and the injected mass can vary with a fixed C_3, then there will be an optimal injected mass that results in the largest delivered mass with the given SEPS. Care should be taken to avoid working with an injected mass that is greater than the optimal injected mass. In this paper, the selected range of launch vehicles does not produce an injected mass greater than an optimal injected mass within the given TOF range.

For the reference payloads targeted (and for significant payload variations about those reference payloads), the "medium" class of launch vehicles provides adequate lift capability. A set of Boeing Delta-IV Medium and Atlas-V Medium launch vehicles were selected for investigation. The two Delta launch vehicles examined included the Delta-IV 4240 and 4450, and the two Atlas cases included the Atlas-V 421 and 431. The resulting delivered payload mass to Saturn with four HTTP I_{sp} 3900-s thrusters is depicted in Fig. 9. First, note that the delivered payload mass increased between consecutive cases averages from 10 to 12%. Second, note the impact that launch-vehicle margins produce, where an 11% performance increase for the Delta-IV 4240 is observed when launch-vehicle margins are reduced from 10 to 2%. The majority of this 11% occurs as a result of the change in launch-vehicle margin, with a smaller portion of this increase caused by increase in duty cycle.

Trajectory Classification and Analysis

Figure 10 presents two trajectories with the same TOF (11.3 year) and R ratio (2:1) but different launch dates for an EVN mission. Because their performances are similar, this indicates that there are two nearly equivalent launch opportunities. Among these two types, the late-type trajectory might deliver slightly less mass, but it uses less onboard propellant. Therefore, the late type is used as the default launch type for further analysis because the required propellant tank is less massive and the operational time of the thruster is shorter.

Because of the flexibility of SEPS in mission design, there are possible launch dates between the early and the late launch dates. Figure 11 shows the performance variation for trajectories with the same TOF (8.5 year) at various launch dates. This figure indicates that a broad launch window exists with less than 10 kg of performance penalty between the early and the late launch date. For the trajectories between the two fully optimal solutions, the launch date is not optimized but given as a fixed input. A similar but more extensive launch date influence for a Mars missions was reported by Williams and Coverstone.[15]

Figure 12 shows three trajectories for an EVN mission with three different R ratios. The TOF of all trajectories in the figure is 9.6 years. It is clear that a spacecraft on the trajectory with the largest R ratio spends the most time thrusting before the flyby occurs. Given the nature of SEPS performance, namely, that orbital energy addition is more efficient near the sun because of greater power availability and control authority, it would seem that spending more time in close proximity to the sun before heading outbound toward the destined target would be beneficial in delivering more mass. However, a larger R-ratio trajectory typically

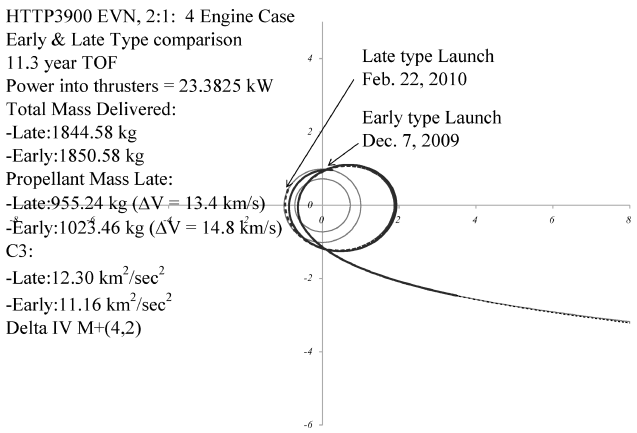

Fig. 10 Trajectories for two launch dates: EVN mission, 11.3-year TOF, 2:1 R-ratio, Delta-IV 4240.

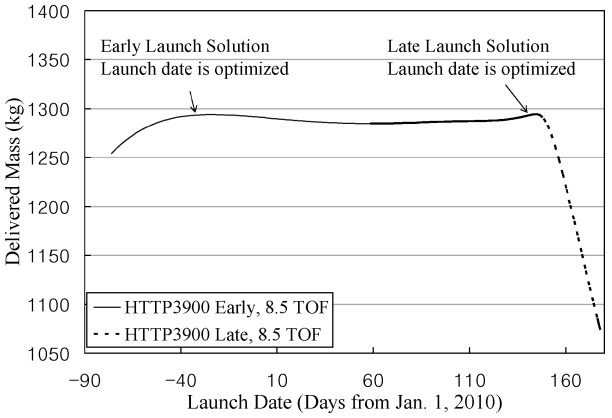

Fig. 11 Delivered mass vs launch date: EVN mission, HTTP 3900 s, 8.5-year TOF, 2:1 R ratio, Delta-IV 4240.

Table 2 Detailed characteristics of EVN trajectories

Time of flight, years	R ratio	Launch date	Cutoff date	Arrival date	C_3, km^2/s^2	Cutoff velocity, km/s
7	2:1	20 June 2010	13 May 2012	20 June 2017	32.69	29.5
	3:1	5 June 2010	11 Dec. 2012	5 June 2017	32.55	32.2
	4:1	9 June 2010	11 July 2013	8 June 2017	35.88	35.6
9.6	2:1	7 May 2010	17 June 2012	13 Dec. 2019	19.37	23.8
	3:1	27 March 2010	19 Jan. 2013	2 Nov. 2019	14.39	25.0
	4:1	12 March 2010	22 March 2013	17 Oct. 2019	15.524	26.3
15	2:1	7 March 2010	19 July 2012	6 March 2025	7.43	20.2
	3:1	11 Feb. 2010	1 Sept. 2012	10 Feb. 2025	9.25	28.6
	4:1	10 Feb. 2010	14 Feb. 2013	10 Feb. 2025	13.43	36.3

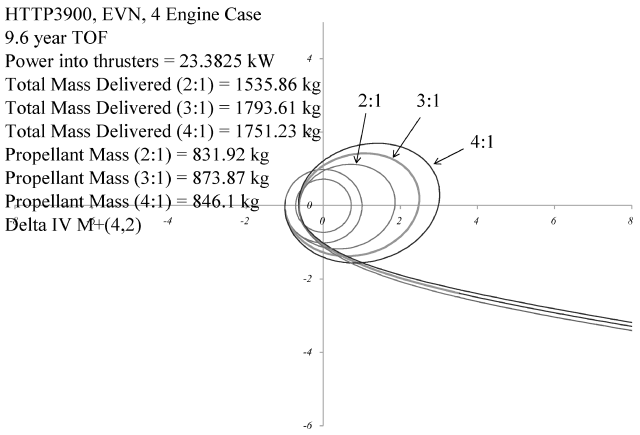

Fig. 12 Trajectories with three different R ratios for an EVN mission, Delta-IV 4240.

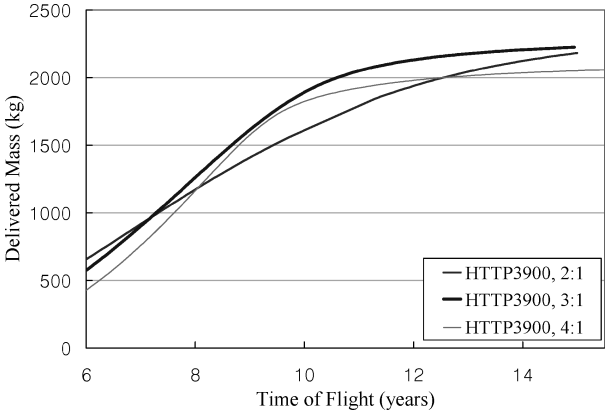

Fig. 13 Delivered mass vs TOF: EVN mission, R-ratio comparison, Delta-IV 4240.

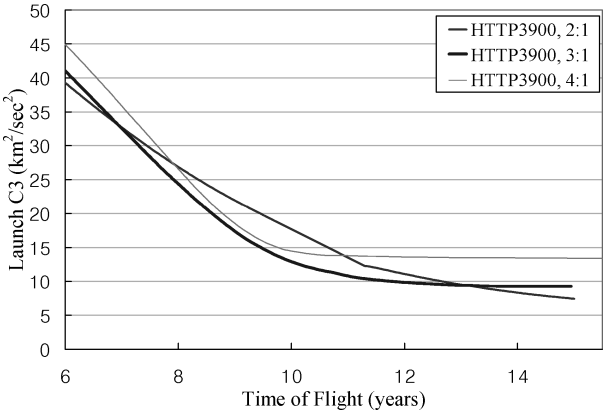

Fig. 14 Launch energy vs TOF: EVN mission, R-ratio comparison, Delta-IV 4240.

needs more launch energy, which in turn means a larger proportion of the total required energy being provided by an inefficient launch vehicle rather than the more efficient low-thrust engine. Tradeoffs between the launch energy and the propellant mass result in an optimal R ratio of 3:1 for this TOF 9.6-year mission.

The optimal R ratio also depends on the TOF of a mission. Figure 13 shows the performances of the three R-ratio trajectories for an EVN mission. At a 7.2-year TOF, the performances of the 2:1 and 3:1 R-ratio trajectories coincide, whereas at an 8.05-year TOF the performances of 2:1 and 4:1 R-ratio trajectories coincide. Smaller R-ratio trajectories are superior in short TOF missions because larger R-ratio trajectories have to spend longer periods of time in flight before the flyby, thereby leaving very little time after the flyby to reach their destination. This constraint forces larger R-ratio trajectories to have lower performance than smaller R-ratio trajectories in short TOF missions.

The performance of 2:1 R-ratio trajectories is similarly superior in longer TOF missions compared to the 4:1 R-ratio trajectories, though for different reasons. In Fig. 14, the launch C_3 plots for the EVN mission are shown. The launch C_3 is larger for the larger R-ratio trajectories for TOF >13 years. This leads to poorer performance for the larger R-ratio trajectories. Onboard propellant usage decreases with increased C_3; however, the initial injected mass also decreases along with the increased C_3. For an EVN mission, the 3:1 R-ratio trajectories are the best performing trajectories for intermediate TOF ($7 \sim 15$ years); however, in general, the best performing R ratio is determined by TOF, the flyby and destination planets, and the characteristics of the SEPS and the launch vehicle. Some characteristics of the different R-ratio trajectories are compared in Table 2. Although not included here, other characteristics, for example, the hyperbolic excess velocity at Venus GA and the allocation of flight time before and after flyby, are important to understanding the R-ratio influence.

Table 2 shows detailed trajectory data at three TOFs for the mission presented in Figs. 13 and 14. The 2:1 R-ratio trajectory has the lowest launch C_3 for a long (15-year) TOF case, whereas the 3:1 R-ratio trajectory has the lowest for an intermediate (9.6-year) TOF case. The lowest C_3 contributes to produce a 3:1 R-ratio trajectory that is superior for the intermediate TOF by injecting the largest mass with the same launch vehicle. The cutoff date in Table 2 is the date when the final thrust phase ends. The cutoff velocity is the heliocentric velocity of the spacecraft at the cutoff date. A larger R-ratio trajectory has a later cutoff date than a shorter R-ratio trajectory with the same TOF. This makes the cutoff velocity faster because the time left to the arrival date is shorter for the larger R-ratio trajectory.

Table 3 shows detailed trajectory characteristics for an EVS mission. The results are similar to Table 2 in trend; however, in general, the launch C_3 variations between the different R-ratio trajectories are larger than in Table 2. The reasons for this contrast are the different total energy increase requirement of the EVS and EVN mission, and the relatively short TOF (2.95, 4.6, and 6 year) of the EVS

Table 3 Detailed characteristics of EVS trajectories

Time of flight, years	R ratio	Launch date	Cutoff date	Arrival date	C_3, km^2/s^2	Cutoff velocity, km/s
2.95	2:1	3 March 2011	11 Nov. 2012	13 Feb. 2014	29.10	25.3
	3:1	20 March 2011	3 May 2013	2 March 2014	39.7	35.3
	4:1	20 May 2011	1 Sept. 2013	2 May 2014	53.6	56.3
4.6	2:1	8 Dec. 2010	21 Jan. 2013	15 July 2015	7.35	17.8
	3:1	8 Nov. 2010	7 Apr. 2013	15 June 2015	7.40	24.5
	4:1	27 Nov. 2010	1 Nov. 2013	4 July 2015	12.85	28.2
6	2:1	1 Nov. 2010	14 Feb. 2013	31 Oct. 2016	2.59	16.2
	3:1	21 Oct. 2010	22 Feb. 2013	21 Oct. 2016	6.21	25.7
	4:1	30 Oct. 2010	23 July 2013	30 Oct. 2016	11.26	36.0

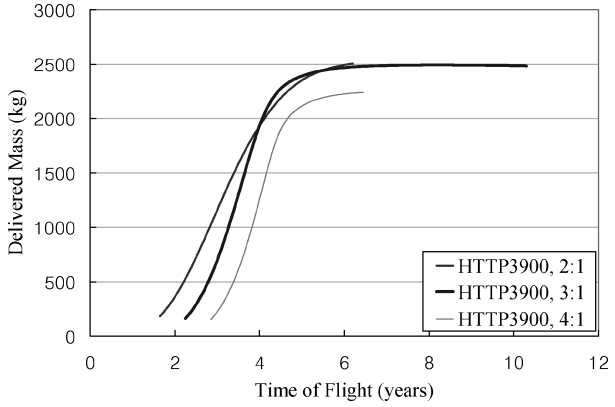

Fig. 15 Delivered mass vs TOF: EVS mission, R-ratio comparison, Delta-IV 4240.

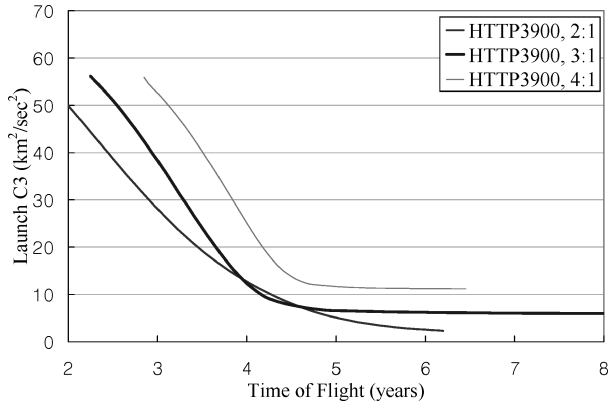

Fig. 16 Launch energy vs TOF: EVS mission, R-ratio comparison, Delta-IV 4240.

mission. The cutoff date is later, and cutoff velocity is higher for larger R-ratio trajectories for all TOF as in EVN missions.

The EVS missions show similar results in an R-ratio analysis. Figures. 15 and 16 show the performances and C_3 of the three R-ratio trajectories for an EVS mission. The 3:1 R-ratio trajectories are superior to 2:1 R-ratio trajectories for intermediate TOF ($4 \sim 5.5$ years) for reasons similar to those of the EVN case, but the performance comparison between 2:1 and 4:1 R-ratio trajectories is different from those of the EVN mission. The reason for this difference is the different total energy increment (launch energy + onboard thrust energy) for each mission. An EVS mission requires a smaller total energy increment than an EVN mission, whereas the C_3 to make an R-ratio trajectory does not differ significantly between the EVS and the EVN mission. This phenomenon produces 4:1 R-ratio trajectories that consistently perform worse than 2:1 R-ratio trajectories in the EVS mission.

In designing an actual mission trajectory, the total operation time of the SEPS should be considered because there is a limitation in total operation time in current SEPS design and the required operation time might be longer than the limit for the state-of-the-art thruster design.[16]

Conclusions

The effect of several mission and systems factors on SEPS delivered mass to outer-planetary destinations has been quantified. The mission factors examined include time of flight, destination, launch vehicle, and trajectory characteristics. The system factors examined include number of thrusters and available power. The performance along with the power variation can be used for solar array and spacecraft sizing to determine the available scientific payload mass.

Multiple optimal trajectories are generated and their characteristics analyzed. Optimal flyby timing for a given mission is also observed. The performance difference between the early and late launch type is not significant, and a relatively wide launch opportunity between the early and late launch that shows consistent performance exists. Finally, total delivered mass estimates to Saturn and Neptune that are feasible with developing SEPS technology are presented.

Acknowledgments

The work described in this paper was performed by Science Applications International Corp. under contract with the NASA Marshall Space Flight Center (MSFC). Special thanks go to Les Johnson, manager of NASA MSFC In-Space Propulsion Technology Investment Projects, and Randy Baggett, manager of NASA MSFC Next Generation Electric Propulsion Technology Area, for providing encouragement and direction for this work.

References

[1]"SEPS Solar Electric Propulsion System Final Review Executive Summary," Lockheed Missiles and Space Co., Inc., LMSC-D758190, Sunnyvale, CA, Jan. 1981.

[2]"Concept Definition and System Analysis Study for Solar Electric Propulsion Stage," Boeing Aerospace Co., DR No. MA-04, Seattle, WA, Jan. 1975.

[3]Rayman, M. D., and Williams, S. N., "Design of the First Interplanetary Solar Electric Propulsion Mission," *Journal of Spacecraft and Rockets*, Vol. 39, No. 4, 2002, pp. 589–595.

[4]Rayman, M. D., Chadbourne, P. A., Culwell, J. S., and Williams, S. N., "Mission Design for Deep Space 1: A Low-Thrust Technology Validation Mission," International Academy of Astronautics, Paper L98-0502, April 1998.

[5]"NASA Research Announcement Proposal Information Package Next Generation Ion Engine Technology," NASA Marshall Space Flight Center, NRA-01-OSS-01 A.9.2, Huntsville, AL, Dec. 2001.

[6]Strange, N. J., and Longuski, J. M., "Graphical Method for Gravity-Assist Trajectory Design," *Journal of Spacecraft and Rockets*, Vol. 39, No. 1, 2002, pp. 9–16.

[7]Sauer, C. G., "Optimization of Multiple Target Electric Propulsion Trajectories," AIAA Paper 73-205, Jan. 1973.

[8]Melbourne, W. G., Richardson, D. E., and Sauer, C. G., "Interplanetary Trajectory Optimization with Power-Limited Propulsion Systems," Jet Propulsion Lab., TR 32-173, California Inst. of Technology, Pasadena, CA, 1962.

[9]Williams, S. N., "An Introduction to the Use of VARITOP A General Purpose Low-Thrust Trajectory Optimization Program," Jet Propulsion Lab., JPL D-11475, California Inst. of Technology, Pasadena, CA, 1994.

[10]Patterson, M., Foster, W. T., Rawlin, J. E., Roman, V., Robert, F., and Soulas, G., "Development Status of a 5/10-kWe Class Ion Engine," AIAA Paper 2001-3489, July 2001.

[11]Kerslake, T., "Photovoltaic Array Performance During an Earth-to-Jupiter Heliocentric Transfer," NASA PS-496, Aug. 2000.

[12]Piñero, L., "Design of a Modular 5-kWe Power Processing Unit for the Next-Generation 40-cm Ion Engine," 27th International Electric Propulsion Conf., IEPC-01-329, Oct. 2001.

[13]"DELTA IV Payload Planners Guide," Boeing Co., MDC 00H0043, Seattle, WA, Oct. 2000.

[14]"Atlas Launch System Mission Planner's Guide Rev. 9," Lockheed Martin, Sunnyvale, CA, Sept. 2001.

[15]Williams, S. N., and Coverstone, V. L., "Mars Missions Using Solar Electric Propulsion," *Journal of Spacecraft and Rockets*, Vol. 37, No. 1, 2000, pp. 71–77.

[16]Sovey, J. S., Rawlin, V. K., and Patterson, M. J., "A Synopsis of Ion Propulsion Development Projects in the United States: SERT I to Deep Space I," NASA TM-1999-209439, 1999.

J. Martin
Associate Editor